

Kinetic Physics 2016 Workshop
Lawrence Livermore National Laboratory, CA, USA
April 5-7, 2016

Vlasov-Fokker-Planck simulation of ion-kinetic effects in ICF implosions

O. Larroche^a

B. Canaud^a, A. Inglebert^a, B.-E. Peigney^a, R. D. Petrasso^b, H. G. Rinderknecht^c,
M. J. Rosenberg^d, V. T. Tikhonchuk^e

^aCEA DIF, 91297 Arpajon CEDEX, France

^bPlasma Science and Fusion Center, MIT, Cambridge, MA 02139, USA

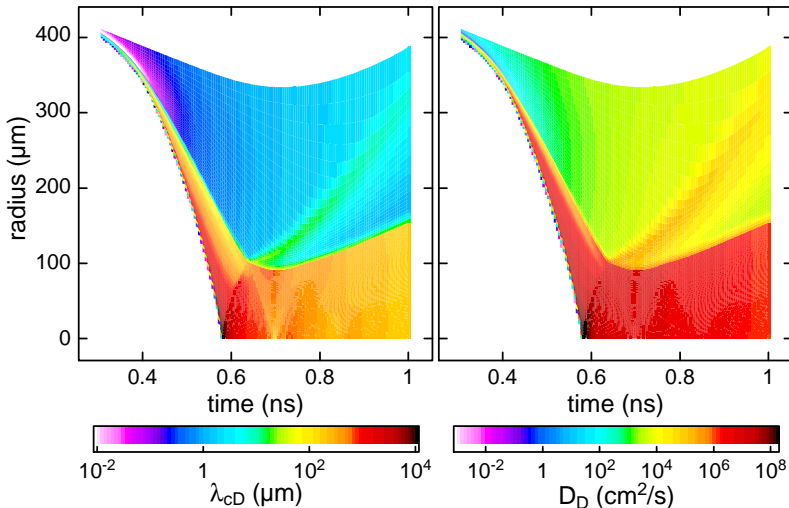
^cLawrence Livermore National Laboratory, Livermore, CA 94550, USA

^dLaboratory for Laser Energetics, University of Rochester, Rochester, NY 14623, USA

^eUniversity of Bordeaux, CNRS, CEA, CELIA, 33405 Talence, France

- Are time and length scales in ICF implosions sufficiently larger than collisional scales ?
 - Hydro simulation post-processing for collisional times, lengths, diffusion coefficients
- Kinetic (Vlasov) formalism with Fokker-Planck ion collision modeling : VFP
 - FPION : hybrid formalism valid on the hydro time scale : kinetic ions, thermal electrons
 - Faster particles are less collisional than thermal bulk : shock fronts
 - Dedicated experiments deviate from hydro modeling, better agreement with VFP
 - Full-scale ICF kinetic and hydro simulations of hot-spot formation show discrepancies
 - Temperature decoupling between ion species in shock-ignition targets.
- Kinetic α -particle transport in igniting ICF targets : Knudsen number ~ 1
 - FUSE : a two-scale ion-kinetic code for ignition
 - First results of FUSE simulation of baseline target : indications of reduced gain
- Work to do :
 - Stratification and/or diffusion or mix at the fuel-pusher interface
 - Ability to treat ion species with large differences in charge and mass
 - Including pusher dynamics in ignition simulations to investigate ignition threshold
 - Need for more quantitative results in longer ignition target calculations

Collisional metrics from hydro simulations



- Implosion of D^3He gas at $\rho = 0.4 \text{ mg/cm}^3$ in a $430 \mu\text{m}$ -radius SiO_2 capsule with a 14.6 kJ, 0.6 ns flat-top laser pulse : hydro simulation post-processing.
- Knudsen number λ_c/L and diffusion coefficient $D = \lambda_c v_{th}$ for a thermal D ion high compared with relevant values $D_{ref} = L^2/T$ where L and T are typical length and time : $L \sim 100 \mu\text{m}$ and $T \sim 200 \text{ ps} \Rightarrow D_{ref} \sim 5 \times 10^5 \text{ cm/s}$ [Larroche *et al*, PoP (2016)]. 3

- Ion Vlasov-Fokker-Planck equation in spherical geometry (in reduced units) :

$$\frac{\partial f_i}{\partial t} + v_r \frac{\partial f_i}{\partial r} + \frac{v_\perp}{r} \left(v_\perp \frac{\partial f_i}{\partial v_r} - v_r \frac{\partial f_i}{\partial v_\perp} \right) + \frac{E_i}{A_i} \frac{\partial f_i}{\partial v_r} =$$

$$\sum_{j=1}^n \left(\frac{\partial f_i}{\partial t} \right)_{ij} + \frac{1}{2\tau_{ei}} \frac{\partial}{\partial v_\alpha} \left[(v_\alpha - u_{i\alpha}) f_i(\mathbf{v}) + \frac{T_e}{A_i} \frac{\partial f_i}{\partial v_\alpha}(\mathbf{v}) \right]$$

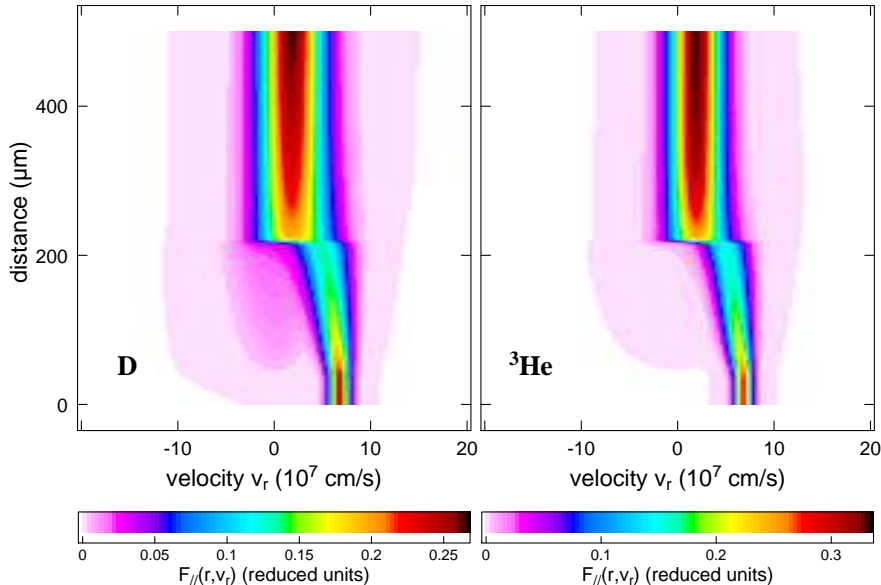
- Coulomb collisions \Rightarrow advection-diffusion in velocity space :

$$\left(\frac{\partial f_i}{\partial t} \right)_{ij} = \frac{4\pi Z_i^2 Z_j^2 \text{Log}\Lambda_{ij}}{A_i^2} \frac{\partial}{\partial v_\alpha} \left[\frac{A_i}{A_j} \frac{\partial \mathcal{S}_j}{\partial v_\alpha} f_i - \frac{\partial^2 \mathcal{T}_j}{\partial v_\alpha \partial v_\beta} \frac{\partial f_i}{\partial v_\beta} \right]$$

with “Rosenbluth potentials” : $\Delta_v \mathcal{S}_j = f_j$, $\Delta_v \mathcal{T}_j = \mathcal{S}_j$

- Coulomb collisions $\Rightarrow \tau_c \sim v^3/n$, several scales, localized metastable states in v space
- Fluid electrons ($\tau \gg \tau_{ee}$), quasineutrality ($L \gg \lambda_D$), ion/hydro timescale ($\tau \gg \omega_{pe}^{-1}$)
 \Rightarrow energy equation left to solve
- Numerical implementation : see [Larroche, PFB \(1993\) – EPJ-D \(2003\)](#)
- Other kinetic simulation tools : LSP (hybrid PIC/fluid) used by [Bellei et al, PoP \(2013, 2014\)](#), VFP code under development : [Taitano et al, JCP \(2015\)](#)

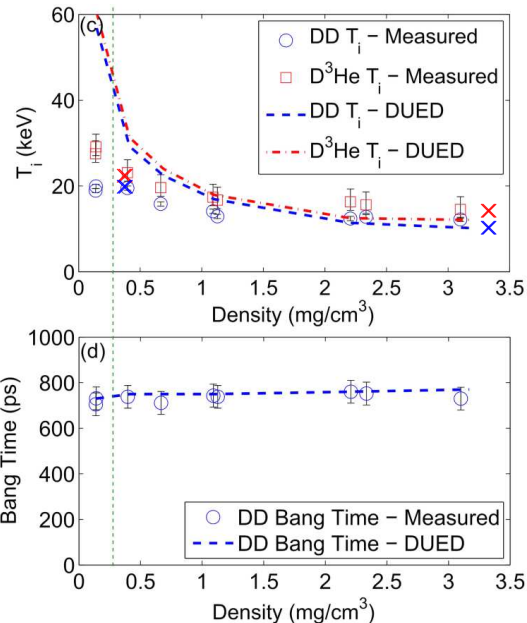
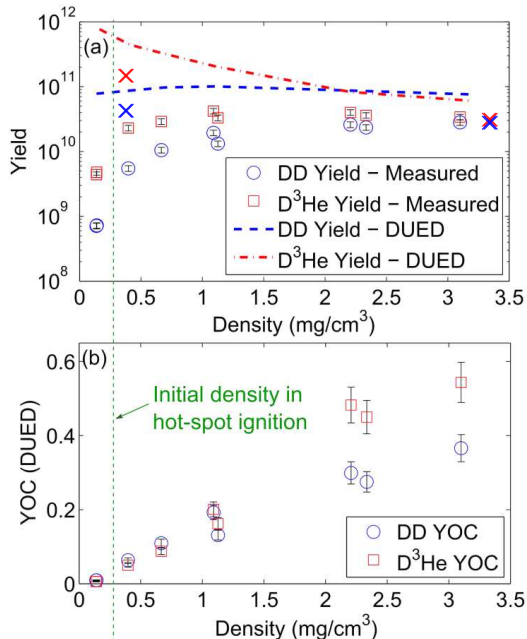
Shock simulations show intrinsically kinetic features



- Asymptotic strong ($M = 5$) shock front in an equimolar D- ${}^3\text{He}$ mixture.
- Maps in phase space (r, v_r) of the longitudinal velocity distribution functions for both ion species [Larroche, PoP (2012)] : notice upstream kinetic features.

- Simulations of high- and low-density cases ($\rho = 3.3$ and 0.4 mg/cm^3).
- Initial condition : Maxwellian distributions for D and ${}^3\text{He}$ at $t = 350 \text{ ps}$.
- Boundary condition on the gas/pusher interface as given by the hydro calculation.
- In the low-density case, the ion temperature T_i for D and ${}^3\text{He}$ is taken from slightly inside the pusher to take into account the (possibly unphysical) large T_i gradient across the interface found in the hydro simulation.
- Numerical grid : 200 cells in r , the spatial grid shrinks or expands to follow the fuel/pusher boundary.
- 128×64 cells in (v_r, v_\perp) space respectively, $\delta v_r = \delta v_\perp$ adjusts as a function of the thermal velocity found in each spatial cell.
- Flux-limited electron thermal conduction with $f = 0.07$.
- Distribution moments, nuclear reactivities and DD-n and D ${}^3\text{He}$ -p reactivity-averaged ion temperatures are computed as a post-processing treatment, using cross-section data from **Bosch & Hale, Nucl. Fusion (1992)**.

A summary of experimental data and simulation results



From Rosenberg *et al* (PRL 2014). \times D^3He - FPION \times DD - FPION

Other observables better rendered as well : reactivity profiles [Larroche *et al* (PoP 2016)]

Hot spot formation in full-scale ICF targets

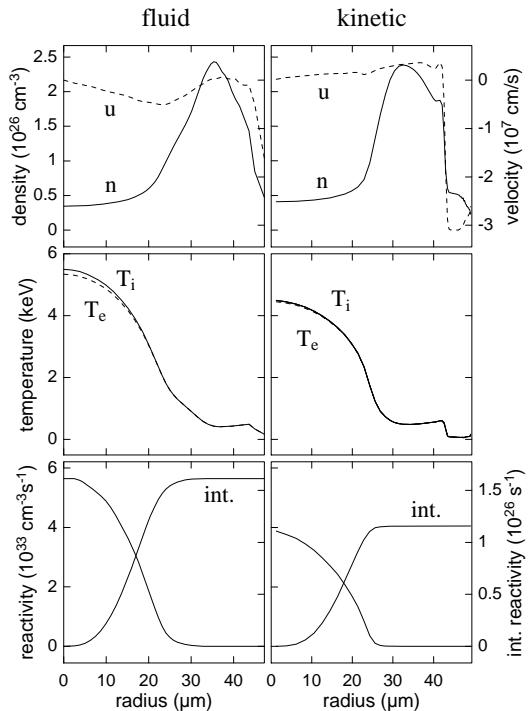
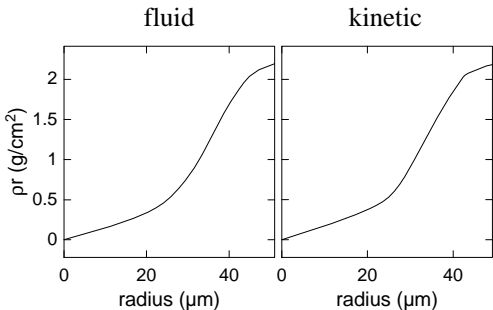
From Larroche, EPJ-D (2003)

- Baseline ICF target near stagnation (17 ns $< t < 17.9$ ns), single species FPION simulation of DT (using $A = 2.5$) :

- Timing modification
- Lower T_i but \approx same ρr profile
- No direct effect on reactivity, but lower $T_i \rightarrow 30\%$ lower reaction rate, although $\phi = \rho r / (\rho r + 6)$ unchanged ?

- Two-species results similar in this stage

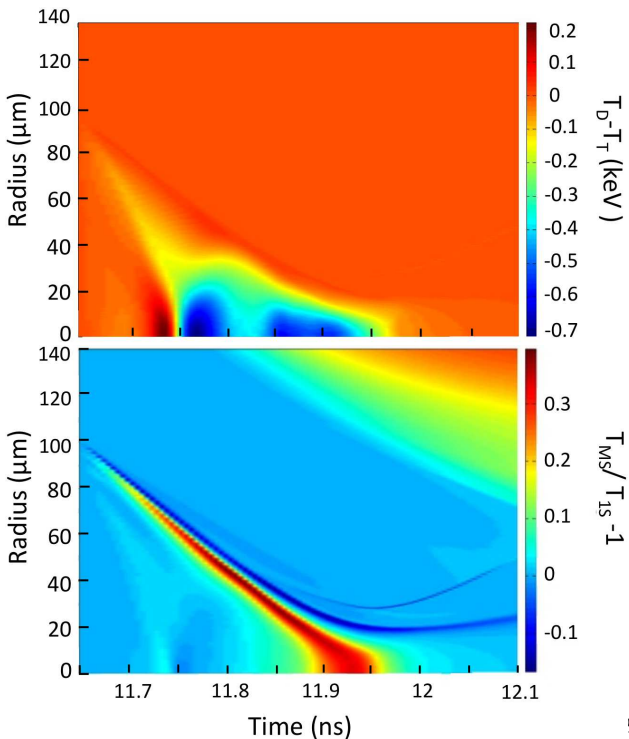
- Longer simulations ?



Temperature decoupling between ion species in ignition-scale targets

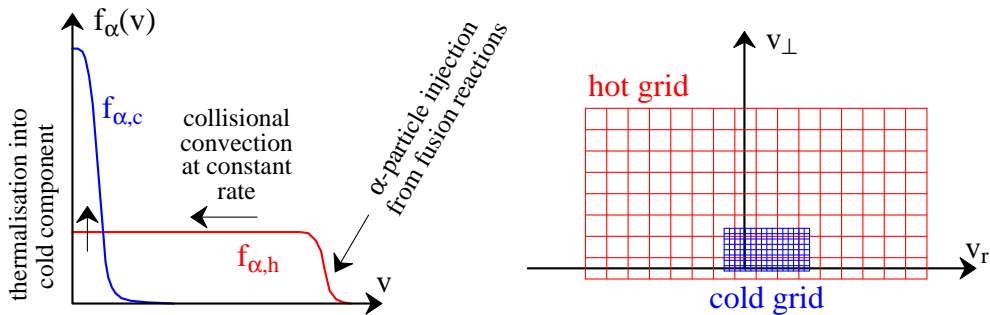
From Inglebert *et al*, EPL (2014) :
very CPU-consuming calculation !

- Shock-ignition target, kinetic effects show up near stagnation.
- Tritium is appreciably hotter than Deuterium in hot spot at stagnation.
- Interpretation :
 $m_i v_{impl}^2 \rightarrow 3k_B \Delta T_i$ before inter-species temperature relaxation.
- Average T_i at stagnation in multi-species calculation larger than T_i in single-species average-ion calculation \rightarrow revisit previous results (Larroche, EPJ-D (2003)).



Kinetic modeling of ignition with fast α -particle treatment

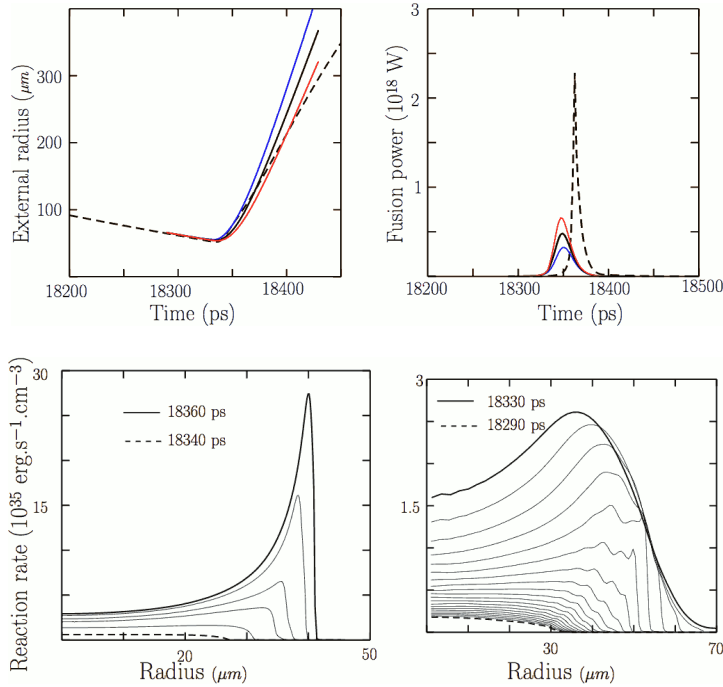
- A new hybrid Fokker-Planck treatment of fast particles has been developed : distributions in the form of the sum of a “cold” component and a “hot” component : $f_a = f_{a,c} + f_{a,h}$
- By construction, the hot component $f_{a,h}$ varies slowly everywhere in velocity space ; it can thus be discretized on a **coarse grid**. From the diffusion (\approx transverse) point of view, $f_{a,h}$ is close to equilibrium, because the source term from nuclear reactions is isotropic.



- Hot \rightarrow hot collisions can be neglected with respect to hot \rightarrow cold ones. Collisions with electrons are treated as usual.
- Implementation : code « FUSE » (Peigney *et al*, JCP (2014)).

Reduced gain in kinetic simulation of baseline target

- First simulations :
Peigney et al, PoP (2014)
 NIF/LMJ-like target with
 code FUSE.
- Pusher modeled by a moving piston with adjustable mass. Interface trajectory :
 - : optimal kinetic
 - : mass $\times 0.5$
 - : mass $\times 2$
 - - - : fluid calculation
- α -particle heating more spread out in space and time, total energy yield $\sim 2 \times$ lower than in hydro + multigroup diffusion calculation.

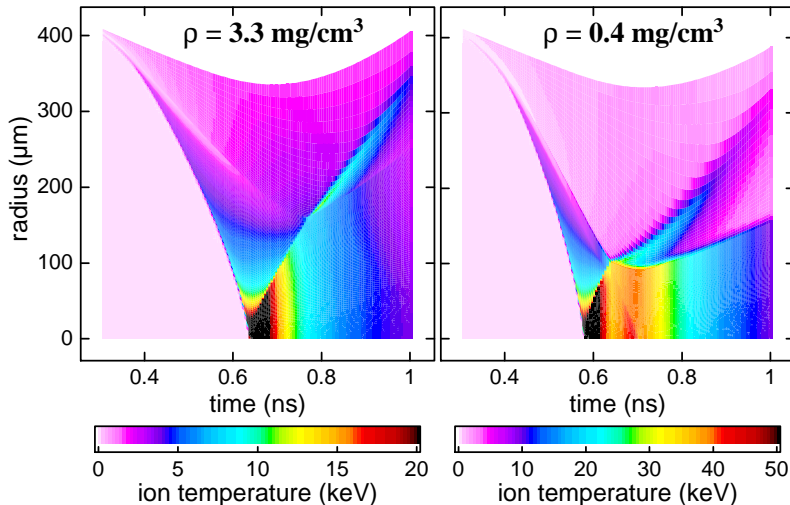


Conclusion and work to do

- Dedicated gas-filled target implosions with moderate to large Knudsen number
 - Moderate K_N : satisfactory agreement between experiments and VFP simulations
 - High K_N : encouraging results, but possible problems at the gas/pusher interface
 - To do : kinetic treatment of diffusion across fuel/pusher boundary
collisional interaction with heavier elements : Si, O
- Hot spot formation in ignition-scale ICF targets
 - Kinetic simulations shows effects on hot-spot T_i and some species decoupling, possibly detrimental to ignition
 - To do : longer simulations including main shock propagation in cold gas
more satisfactory treatment of other physics is needed
- Kinetic effects on ignition and burn
 - New kinetic code treats α -particle transport and thermalization
 - First proof-of-principle simulation results show lower gain
 - To do : extensive quantitative simulations of ignition (threshold ?) and burn
same improvements as above are needed

References

- C. Bellei *et al*, Phys. Plasmas **20**, 012701 (2013).
- C. Bellei *et al*, Phys. Plasmas **21**, 056310 (2014).
- H.-S. Bosch, G. M. Hale, Nucl. Fusion **32**, 611 (1992).
- A. Inglebert, B. Canaud, O. Larroche, Europhys. Lett. **107**, 65003 (2014).
- O. Larroche, Phys. Fluids B **5**, 2816 (1993).
- O. Larroche, Eur. Phys. J. D **27**, 131 (2003).
- O. Larroche, Phys. Plasmas **19**, 122706 (2012).
- O. Larroche *et al*, Phys. Plasmas **23**, 012701 (2016).
- B. Peigney, O. Larroche, V. T. Tikhonchuk, J. Comput. Phys. **278**, 416 (2014).
- B. Peigney, O. Larroche, V. T. Tikhonchuk, Phys. Plasmas **21**, 122709 (2014).
- M. J. Rosenberg *et al*, Phys. Rev. Lett. **112**, 185001 (2014).
- M. J. Rosenberg *et al*, Phys. Plasmas **22**, 062702 (2015).
- W. T. Taitano *et al*, J. Comput. Phys. **297**, 357 (2015).



- Large T_i jump across the pusher/fuel interface in the low-density case [Rosenberg *et al*, PoP (2015) - Larroche *et al*, PoP (2016)]

VFP equation in spherical geometry, to lowest order in m_e/m_i , for species i :

$$\frac{\partial f_i}{\partial t} + v_r \frac{\partial f_i}{\partial r} + \frac{v_\perp^2}{r} \frac{\partial f_i}{\partial v_r} - \frac{v_\perp v_r}{r} \frac{\partial f_i}{\partial v_\perp} + \frac{\mathcal{E}_i}{A_i} \frac{\partial f_i}{\partial v_r} = \sum_{j=1}^n \left(\frac{\partial f_i}{\partial t} \right)_{ij} + \left(\frac{\partial f_i}{\partial t} \right)_{ie}$$

A_i mass number of species- i ions ; electron-ion collision term :

$$\left(\frac{\partial f_i}{\partial t} \right)_{ie} = \frac{1}{2\tau_{ei}} \frac{\partial}{\partial v_\alpha} \left[(v_\alpha - u_{i\alpha}) f_i(\vec{v}) + \frac{T_e}{A_i} \frac{\partial f_i}{\partial v_\alpha}(\vec{v}) \right]$$

with electron-ion collision time

$$\tau_{ei} = \frac{3\sqrt{\pi} A_i T_e^{3/2}}{2\epsilon\sqrt{2} Z_i^2 n_e \text{Log}\Lambda_{ie}}$$

$\epsilon = \sqrt{m_e/m_p}$ (m_e, m_p : electron and proton masses), Z_i charge number of species- i ions, n_a, \vec{u}_a, T_a : density, velocity and temperature of species a , $\text{Log}\Lambda_{ab}$ Coulomb logarithm for collisions between species- a and - b particles, effective electric field :

$$\mathcal{E}_i = -\frac{Z_i}{n_e} \frac{\partial P_e}{\partial r}$$

P_e : electron pressure. Units used are :

$$\text{time} : \tau_0 = \frac{(k_B T_0)^{3/2} m_p^{1/2}}{4\pi e^4 n_0} \quad , \quad \text{space} : \lambda_0 = \left(\frac{k_B T_0}{m_p} \right)^{\frac{1}{2}} \tau_0$$

$k_B T_0$ and n_0 are given reference values of the thermal energy per particle and number density, e is the elementary charge.

$$n_e = \sum_{j=1}^n Z_j n_j \quad , \quad u_e = \frac{1}{n_e} \sum_{j=1}^n Z_j n_j u_j \quad , \quad \tilde{Z} = \frac{\sum_{j=1}^n Z_j^2 n_j \text{Log}\Lambda_{ej}}{n_e \text{Log}\Lambda_{ee}}$$

$$\text{Log}\Lambda_{ab} = \text{Log} \frac{\lambda_D}{\max(\lambda_{bar}, \rho_\perp)} \quad \text{where} \quad \lambda_D = \frac{\lambda_{D0}}{\lambda_0} \left(\frac{n_e}{T_e} + \sum_{j=1}^n \frac{n_j Z_j^2}{T_j} \right)^{-1/2}$$

$$\lambda_{D0} = \left(\frac{k_B T_0}{4\pi n_0 e^2} \right)^{1/2} = \text{reference Debye length} ; \quad \rho_\perp = \left(\frac{\lambda_{D0}}{\lambda_0} \right)^2 \frac{Z_a Z_b}{A_{ab} u^2}$$

$$\lambda_{bar} = \frac{\hbar}{\tau_0 k_B T_0} \frac{1}{A_{ab} u} \quad \text{where} \quad A_{ab} = \frac{A_a A_b}{A_a + A_b} \quad \text{and} \quad u = \sqrt{3} \left(\frac{T_a}{A_a} + \frac{T_b}{A_b} \right)^{1/2}$$

Collision term between ions of species i and j :

$$\left(\frac{\partial f_i}{\partial t} \right)_{ij} = \frac{4\pi Z_i^2 Z_j^2}{A_i^2} \text{Log}\Lambda_{ij} \frac{\partial}{\partial v_\alpha} \left[\frac{A_i}{A_j} \frac{\partial \mathcal{S}_j}{\partial v_\alpha} f_i - \frac{\partial^2 \mathcal{T}_j}{\partial v_\alpha \partial v_\beta} \frac{\partial f_i}{\partial v_\beta} \right]$$

Rosenbluth potentials \mathcal{S}_j and \mathcal{T}_j :

$$\mathcal{S}_j = -\frac{1}{4\pi} \int \frac{f_j(\vec{v}')}{|\vec{v} - \vec{v}'|} d^3v' \quad \text{and} \quad \mathcal{T}_j = -\frac{1}{8\pi} \int |\vec{v} - \vec{v}'| f_j(\vec{v}') d^3v'$$

→ Poisson equations in velocity space : $\Delta_v \mathcal{S}_j = f_j$ and $\Delta_v \mathcal{T}_j = \mathcal{S}_j$ with appropriate boundary conditions.

Electron temperature T_e from conservation of electron thermal energy density W_e :

$$\begin{aligned} \frac{\partial W_e}{\partial t} + \frac{1}{r^2} \frac{\partial}{\partial r} (r^2 u_e W_e) + \frac{1}{r^2} \frac{\partial}{\partial r} (r^2 u_e) P_e - \frac{1}{r^2} \frac{\partial}{\partial r} \left(r^2 \kappa_e \frac{\partial T_e}{\partial r} \right) &= \\ &= \sum_{j=1}^n \frac{3n_j}{2\tau_{ej}} (T_j - T_e) + \left(\frac{\partial W_e}{\partial t} \right)_{rad} \end{aligned}$$

κ_e : Spitzer-Härm electron thermal conduction in multi-ion-species case :

$$\kappa_e \approx \frac{64\sqrt{2}\delta_T(\tilde{Z})}{\sqrt{\pi}} \frac{T_e^{5/2}}{\epsilon \tilde{Z} \text{Log} \Lambda_{ee}}$$

W_e and P_e from electron fluid equation of state, with low-density limit :

$$W_e(n_e, T_e) \xrightarrow[n_e \rightarrow 0]{} \frac{3}{2} n_e T_e \quad ; \quad P_e(n_e, T_e) \xrightarrow[n_e \rightarrow 0]{} n_e T_e$$

Electron EOS takes Fermi degeneracy into account through :

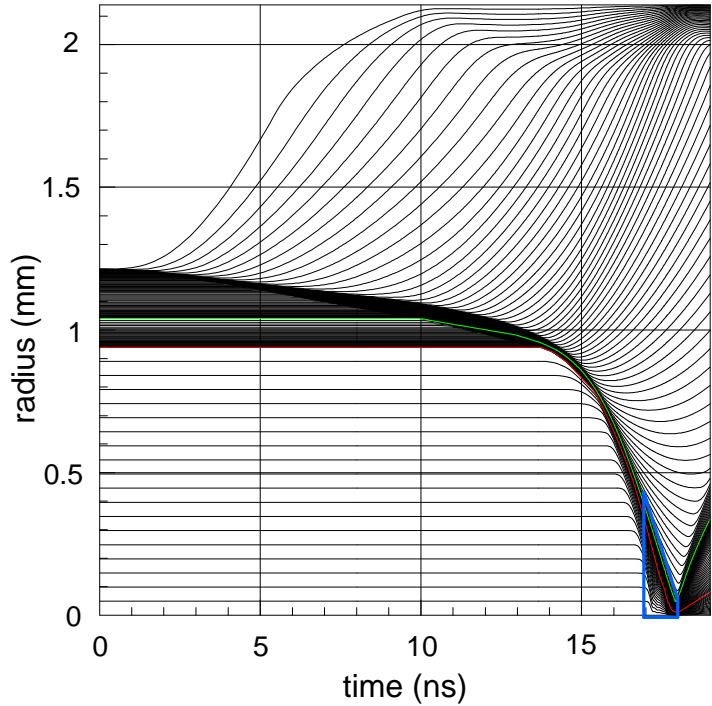
$$n_e = 4\pi \left(\frac{2m_e k_B T_e}{h^2} \right)^{3/2} I_{1/2}(z) \quad ; \quad W_e = \frac{3}{2} P_e = 4\pi \left(\frac{2m_e k_B T_e}{h^2} \right)^{3/2} k_B T_e I_{3/2}(z)$$

“Fermi integrals” $I_{n/2}(z) = \int_0^\infty \frac{y^{n/2}}{z^{-1}e^y + 1} dy$

Bremsstrahlung losses :

$$\left(\frac{\partial W_e}{\partial t} \right)_{rad} = -P_{rad} = -4.14 \times 10^{-4} T_0(\text{keV}) n_e T_e^{1/2} \sum_i n_i Z_i^2$$

- Green : DT/pusher interface
- Red : initial interface solid DT/DT gas
- Blue : kinetic treatment region



Backup : Fusion emissivities in exploding-pusher gas-filled targets

Reaction rate :

$$R_{ij}(r, t)$$

Emissivity :

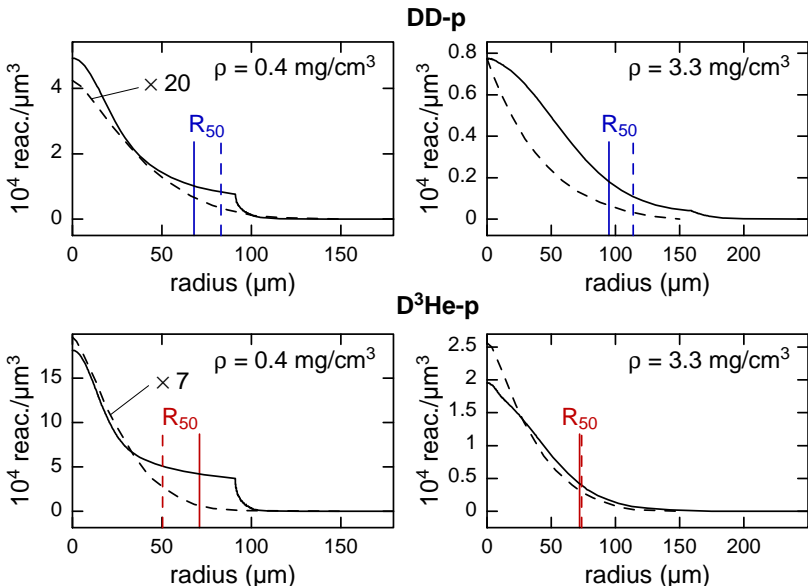
$$E_{ij}(r) = \int_{-\infty}^{\infty} R_{ij}(r, t) dt$$

Yield :

$$Y_{ij} = \int_0^{\infty} E_{ij}(r) 4\pi r^2 dr$$

Median Radius :

$$0.50 \times Y_{ij} = \int_0^{R_{50}} E_{ij}(r) 4\pi r^2 dr$$

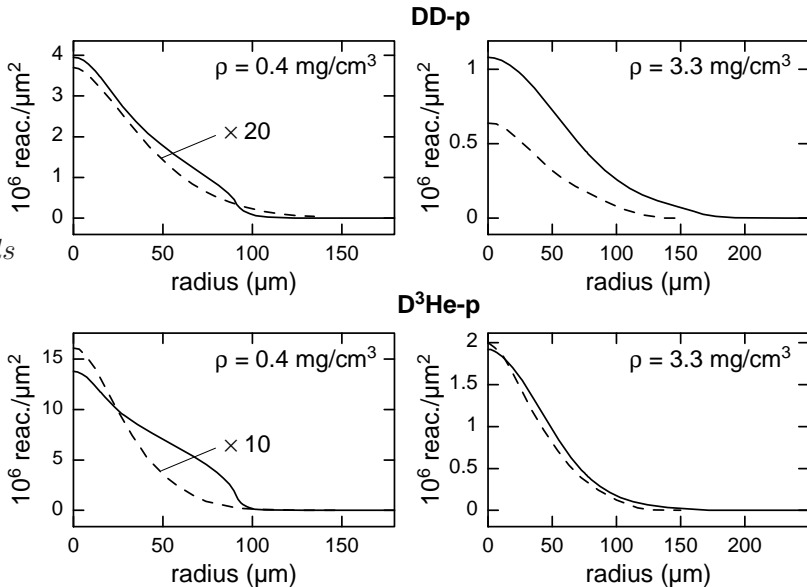
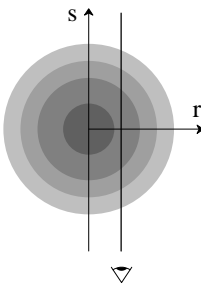


— : FPION calculation of D^3He gas-filled target implosions
 [Larroche *et al*, PoP (2016)]
 - - - : Measured profiles [Rosenberg *et al*, PoP (2015)]

Backup : Fusion surface brightness in exploding-pusher targets

Surf. brightness :

$$B_{ij}(r) = \int_{-\infty}^{\infty} E_{ij}(\sqrt{r^2 + s^2}) ds$$



— : FPION calculation of D^3He gas-filled target implosions
 [Larroche *et al*, PoP (2016)]

— — — : Measured profiles [Rosenberg *et al*, PoP (2015)]